Journal of Physics: Conference Series **641** (2015) 012027 doi:10.1088/1742-6596/641/1/012027

Gravitational disturbances generated by the Sun, Phobos and Deimos in orbital maneuvers around Mars with automatic correction of the semi-major axis

E M Rocco

National Institute for Space Research – INPE, Space Mechanics and Control Division, São José dos Campos, SP-Brazil

E-mail: evandro.rocco@inpe.br

Abstract. The objective of this work is to analyze orbital maneuvers of a spacecraft orbiting Mars, considering disturbance effects due to the gravitational attraction of the Sun, Phobos and Deimos, beyond the disturbances due to the gravitational potential of Mars. To simulate the trajectory, constructive aspects of the propulsion system were considered. Initially ideal thrusters, capable of applying infinite magnitude of the thrust, were used. Thus, impulsive optimal maneuvers were obtained by scanning the solutions of the Lambert's problem in order to select the maneuver of minimum fuel consumption. Due to the impossibility of applying an impulse, the orbital maneuver must be distributed in a propulsive arc around the position of the impulse given by the solution of the Lambert's problem. However the effect of the propulsive arc is not exactly equivalent to the application of an impulse due to the errors in magnitude and direction of applied thrust. Therefore, the influence of the thrusters' capacity in the trajectory was evaluated for a more realistic model instead of the ideal case represented by the impulsive approach. Beyond the evaluation of the deviation in the orbital path, was considered an automatic correction of the semi-major axis using continuous low thrust controlled in closed loop to minimize the error in the trajectory after the application of the main thrust.

1. Introduction

This study aims to evaluate the influence of the gravitational attraction of the Sun, Phobos and Deimos, beyond the disturbances due to the gravitational potential of Mars, during orbital maneuvers of a spacecraft orbiting Mars. Some constructive aspects of the propulsion system were considered. Initially ideal thrusters, capable of applying infinite magnitude of the thrust, were used. Thus, impulsive optimal maneuvers were obtained by scanning the solutions of the Lambert's problem (Two Point Boundary Value Problem) for various values of transfer time in order to select the maneuver of minimum fuel consumption [1]. Then, the selected maneuver was simulated considering a more realistic model of the propulsion system. In fact is not possible to accomplish an impulsive maneuver because to perform this kind of maneuver it would be necessary an infinite capacity for the thrusters, because the entire velocity change of the spacecraft should occur instantly. Thus, the orbital maneuver must be distributed in a propulsive arc around the position of the impulse given by the solution of the Lambert's problem. In this arc was used a continuous thrust, limited to the capacity of the thrusters. However the effect of the propulsive arc is not exactly equivalent to the application of an impulse due to the errors in magnitude and direction of applied thrust. The difference between these approaches produces a deviation in the trajectory. The evaluation of deviation is extremely relevant in the mission

analysis and spacecraft design of the trajectory control system. Therefore, the influence of the capacity of thrusters in the trajectory was evaluated for a more realistic model instead of the ideal case represented by the impulsive approach. So initially the bi-impulsive maneuver, which consists of finding the transfer orbit that connects a point on the initial orbit to another point in the final orbit spending a certain amount of time, is accomplished. An algorithm for solving this problem by universal variables was used [1] [2]. Then, the optimum maneuver is selected and simulated using the Spacecraft Trajectory Simulator (STRS) [3] [4] [5]. In the STRS simulation environment, the orbital movement is obtained by the solution of Kepler's equation for each simulation step. Thus, given an initial state, the Keplerian elements are obtained and propagated to the next step, to be converted into the new state. In the STRS simulator, the reference state is defined by guidance subsystem providing the ideal trajectory to be followed, according to the solution of the Lambert's problem. This reference is continuously compared with the current position of the vehicle generating an error signal, which is inserted into porporcional-integral-derivative controller, generating a signal capable of reducing errors in transition and stationary regimes. This signal is sent to the actuators to generate a signal to be applied in the dynamics model of the movement, added to the disturbing signal due to the gravitational forces of the Sun, Phobos and Deimos. Therefore, the evolution of the vehicle can be analyzed.

2. Orbital perturbation

The evaluation of the errors in the trajectory becomes even more relevant if the effects of orbital perturbations acting on the vehicle were considered. Thus, deviations in the trajectory due to disturbances caused by the Mars gravitational potential and the gravitational attractions of the Sun, Phobos and Deimos were included in the simulations, since all these perturbations models are available in the orbital simulator STRS. The mathematical models of these perturbations in the motion of a spacecraft can be found in [6] and [7]. A short discussion of the environmental perturbations considered in this work is presented below.

2.1. Mars gravitational potential

Considering two particles of mass m and M ($M >>> m$) separated by a distance r, the acceleration $\vec{a}_m$ of the mass m in relation to the center of mass of the particles, is given by:

$$\vec{a}_m = -\frac{GM}{r^3}\vec{r} \tag{1}$$

where G is the universal gravitational constant ($G = 6{,}6726 \pm 0{,}0005 \times 10^{-11}$ m^3/kg s^2), $\vec{r}$ is the vector connecting the two particles, $\vec{a}_m$ is the acceleration vector in the direction of $\vec{r}$. The vector $\vec{a}_m$ can be obtained by the gradient of the gravitational potential U.

$$\vec{a}_m = \vec{\nabla} U\,; \quad U = \frac{GM}{r} = \frac{\mu}{r}\,; \quad F = \frac{\partial U}{\partial r} = -\frac{\mu}{r^2} \tag{2}$$

From the second derivative of U with respect to the coordinates x, y and z the Laplace equation can be obtained.

$$\nabla^2 U = \frac{\partial^2 U}{\partial x^2} + \frac{\partial^2 U}{\partial y^2} + \frac{\partial^2 U}{\partial z^2} \quad \Rightarrow \quad \nabla^2 U = \mu\left[-\frac{3}{r^3} + \frac{3\left(x^2+y^2+z^2\right)}{r^5}\right] = 0 \tag{3}$$

Using spherical coordinates, the solution of the Laplace's equation is given by Eq. (4):

$$U = \sum_{n=0}^{\infty}\sum_{m=0}^{n} \frac{1}{r^{n+1}} P_{nm}(\operatorname{sen}\phi)\left[\begin{matrix} C_{nm}\cos(m\lambda) + \\ + S_{nm}\operatorname{sen}(m\lambda)\end{matrix}\right]; \quad P_{nm}(s) = \left(1-s^2\right)^{m/2}\frac{\mathrm{d}^m}{\mathrm{d}\,s^m}P_n(s); \quad P_{nm}(s) = 0 \text{ for } m > n \tag{4}$$

$$P_n(s) = \frac{1}{2^n}\sum_{j=0}^{N}\frac{(-1)^j(2n-2j)!\,s^{n-2j}}{j!(n-j)!(n-2j)!}; \quad N = \frac{n}{2} \text{ for even } n; \quad N = \frac{n-1}{2} \text{ for odd } n; \quad n = 0, 1, 2,\ldots \tag{5}$$

where C_{nm}, S_{nm} are constant coefficients that represent the spherical harmonics; ϕ is the Mars-centric latitude; λ is the Mars-centric longitude; $P_{nm}(s)$ are the Legendre associated functions for degree n and order m; $P_n(s)$ are the Legendre polynomials and $s = \operatorname{sen}\phi$. In this work was used the Goddard Mars model 2B. This gravitational model has been developed from data of NASA's missions [8] [9]. The maximum degree and order capable to be considered by this model is 80.

2.2. Gravitational attractions of the Sun, Phobos and Deimos

The gravitational potential due to the presence of a third celestial body is given by Eq. (6) [6]:

$$F' = \left(\frac{\mu'}{r'}\right)\left[1 + \sum_{n=2}^{\infty}\left(\frac{r}{r'}\right)^n P_n \cos\psi\right] \tag{6}$$

where: μ' is obtained by the product of the gravitational constant and the mass m' of the third body; r' is the absolute position vector of the third body related to the center of Mars; ψ is the angle between the position vector of the satellite related to the Mars $\vec{r}$ and the position vector of the satellite related to the third body; r is the absolute position vector of the satellite related to the Mars. Basically the gravitational perturbations produce variations in the right ascension of the ascending node and variations in the argument of perigee. According to [10] the general problem of three bodies provides a simple way to calculate the disturbing accelerations due to the gravitational attraction of the bodies, obtained from the Newton's law of gravitation:

$$\ddot{\vec{r}}_1 = -G\,m_2\frac{\vec{r}_1 - \vec{r}_2}{|\vec{r}_1 - \vec{r}_2|^3} + G\,m_3\frac{\vec{r}_3 - \vec{r}_1}{|\vec{r}_3 - \vec{r}_1|^3};\quad \ddot{\vec{r}}_2 = -G\,m_3\frac{\vec{r}_2 - \vec{r}_3}{|\vec{r}_2 - \vec{r}_3|^3} + G\,m_1\frac{\vec{r}_1 - \vec{r}_2}{|\vec{r}_1 - \vec{r}_2|^3};\quad \ddot{\vec{r}}_3 = -G\,m_1\frac{\vec{r}_3 - \vec{r}_1}{|\vec{r}_3 - \vec{r}_1|^3} + G\,m_2\frac{\vec{r}_2 - \vec{r}_3}{|\vec{r}_2 - \vec{r}_3|^3} \tag{7}$$

where $\vec{r}_1$, $\vec{r}_2$ and $\vec{r}_3$ are the positions of the bodies, m_1, and m_3 the masses of the bodies.

3. Results

Due to the impossibility of application of an infinite thrust the maneuver must be distributed in a propulsive arc around the position of the impulse. In this propulsive arc continuous thrust is applied, limited to the capacity of the thrusters. However, the effect is not equivalent to the application of an impulse. According to [6] the velocity increment applied to the spacecraft is given by Eq. (8):

$$\Delta V = g_0 I_{sp} \ln\frac{m_i}{m_f} - \int_{t_1}^{t_2} g \sin\gamma \,\mathrm{d}t \tag{8}$$

where g_0 is the gravitational constant at planet's surface and g at the spacecraft altitude, I_{sp} is the specific impulse, γ is the flight angle formed between the direction of the velocity and the thruster pointing direction, m_i is the mass of the vehicle and m_f the final mass. From Eq. (8) it is verified that the distribution of the maneuver in an arc produces a reduction in the applied velocity increment if the direction of application of the thrust remain constant, since in this case the angle γ is different than zero. To minimize this effect the flight angle could be maintained near to zero by controlling the pointing direction of the thruster, ensuring that the thrust is always applied in the direction tangential to the path. However, this solution is more complex because it requires the use of the attitude control system, and in fact, this approach is not capable to reduce the error in the final orbit reached by the vehicle. To optimize the propulsive maneuvers distributed in arcs, it must be considered the optimization procedure for orbital maneuvers with continuous thrust: [11]. However the optimization of maneuvers with continuous thrust is a difficult task, since in most of the cases it requires numerical methods and the definition of initial values for obtaining the solution. Thus, a simple possibility to minimize the effect caused by the error in the thrust direction would be executing the maneuver in several stages, each one applying just a fraction of the total velocity increment, to reduce each

propulsive arc and thereby reduce the angle γ. In this case the error in the trajectory is minimized but the total time spent to reach the final orbit is maximized, characterizing a problem of multi-objective optimization with conflicting objectives. Some studies of multi-objective problems applied to orbital trajectories can be found in [12]. Another possibility to minimize the error in the trajectory after the application of the main thrust could be the use of an automatic correction of the orbital elements using continuous low thrust controlled in closed loop, as presented by [7]. In this approach, the final orbital elements are defined, then control loops for each of these elements determine, at each step of the simulation, the magnitudes and directions of application of thrust necessary to reach the desired orbital elements. The variations of elements occur gradually until the difference between the current and reference signals do not generate errors. Then, the propulsion system is turned off automatically. To illustrate the necessity of split the maneuver in several propulsive arcs, or use the automatic correction approach, six cases are presented: case 1 for impulsive approach, with the thrust applied during 1s; cases 2 to 6 for maneuvers using thruster with capacity of 150 N to 350 N, with and without the automatic correction. The initial orbit is defined by the following keplerian elements: a = 4000 km, e = 0.001; i = 10º; Ω = 55º; ω = 25°. The final orbit is defined by: a = 5000 km, e = 0.001; i = 10º; Ω = 55º; ω = 25º. The time interval necessary to perform the transfer maneuver and the necessary velocity increment, were determined by the Lambert's problem (case 1): t = 4583 s; Δv_1 = 176.988 m/s ($\Delta\vec{v}_1 = -175.174\hat{i} - 0.226\hat{j} + 25.279\hat{k}$); Δv_2 = 167.368 m/s ($\Delta\vec{v}_2 = 165.656\hat{i} + 0.525\hat{j} - 23.874\hat{k}$).

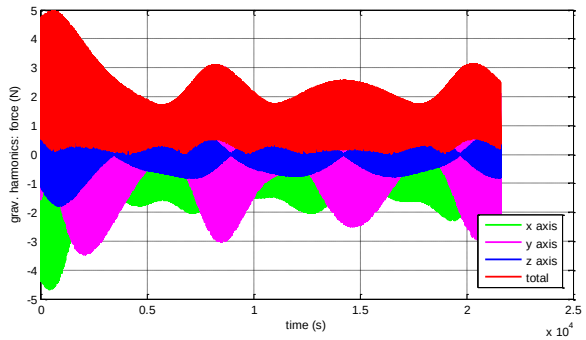

Figure 1. Mars gravitational potential disturbing applied during the maneuver

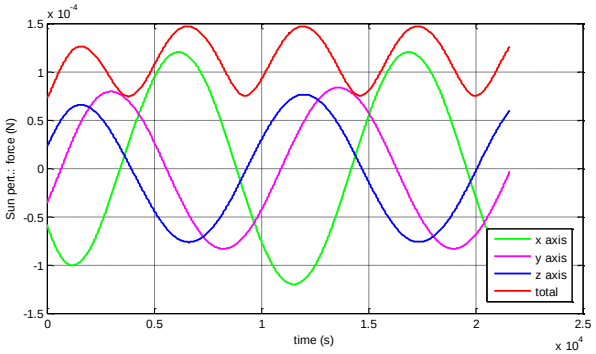

Figure 2. Sun gravitational disturbing applied during the maneuver

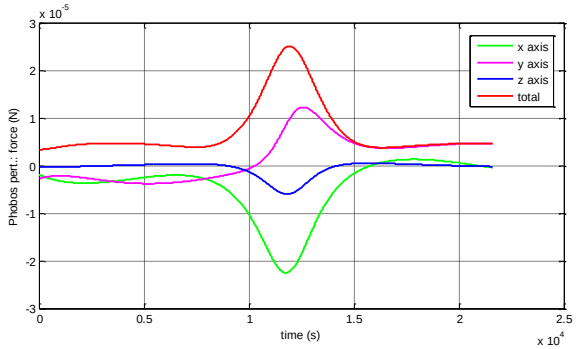

Figure 3. Phobos gravitational disturbing applied during the maneuver

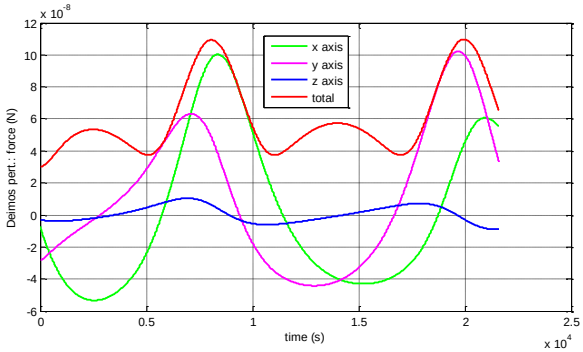

Figure 4. Deimos gravitational disturbing applied during the maneuver

The gravitational disturbing forces acting on the spacecraft during the maneuver are shown in Figs. 1 to 4. It can be verified that the major gravitational disturbing force is produced by the Mars gravitational potential. The influence of the Phobos and Deimos is not so relevant due to the small mass of the Mars's satellites. Although the influence of Phobos could be relevant if the spacecraft trajectory become too close of Phobos, since the orbit of Phobos is not too high.

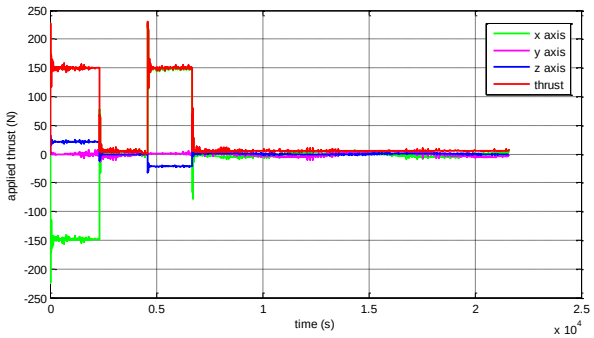

Figure 5. Case 2 (150N): applied thrust with automatic correction

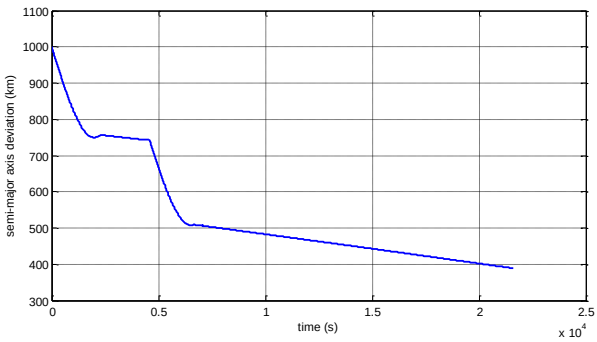

Figure 6. Case 2 (150N): semi-major axis error with automatic correction

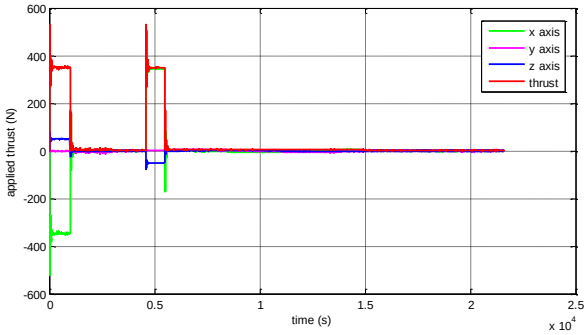

Figure 7. Case 6 (350N): applied thrust with automatic correction

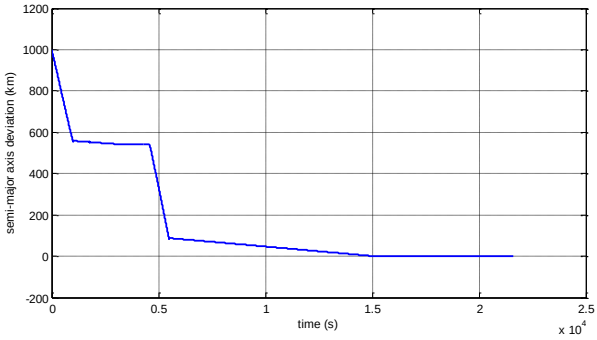

Figure 8. Case 6 (350N): semi-major axis error with automatic correction

The cases 1 to 6, taken into account several thrust capacities, some of them were shown in the previous figures. The error and the velocity increment for all cases are summarized in Table 1.

Table 1. Semi-major axis error and total applied velocity increment

	Semi-Major Axis Error (km)		Total Velocity Increment (m/s)	
Thrust Capacity	without automatic correction	with automatic correction	without automatic correction	with automatic correction
Case 1: Impulsive	0.00597855	0.00368516	353.516082	353.294809
Case 2: 150 N	526.228288	389.124696	359.442515	395.694899
Case 3: 200 N	316.722898	165.359838	359.130541	398.331927
Case 4: 250 N	207.462009	47.949564	361.249271	400.715093
Case 5: 300 N	145.138706	**0.0001561**	361.021206	397.495559
Case 6: 350 N	106.691771	0.0024326	363.167535	388.512041

When considered the application of the impulses, in case 1, all the velocity increment and all change in the semi-major axis are performed instantly. Therefore the applied thrust is in fact a pulse, however the continuous thrust was applied to counteract the disturbances. This continuous thrust was applied because the STRS was adjusted to control the trajectory, reducing the effect produced by the disturbances, but the main orbital maneuver in case 1 was performed in an impulsive way. From Table 1 can be verified that this case produces a small error in the final semi-major axis of the orbit. Both results, considering automatic correction and without automatic correction, presented very small errors, around 5 meters. Cases 2 to 4 in general presented results with bigger error. In these cases the change in the semi-major axis occurs gradually. When using the automatic correction the error was continually reduced after the application of the main thrust, nevertheless the amount of time available to correct the trajectory was not enough, since the thrust capacity adjusted for the automatic correction

was 5N. With more time or with higher thrust capacity the results obtained for cases 2 to 4 could be improved. Thus, in a mission analysis and in the dimensioning of a spacecraft should be considered all possible combinations of the main thrust and the thrust capacity used in the automatic correction, to choose the best solution for the mission. In this study the best result was obtained in case 5 considering the main capacity of 300N. Without the automatic correction, the semi-major axis error was 145.13 km. However with the automatic correction the error was reduced to 15.61 cm. This result is much better than the results obtained in the other cases, even considering the impulsive approach. The performance of the automatic correction was able to correct the errors generated by the fact that the main thrust was distributed in a propulsive arc instead of an impulse applied instantly. With this new procedure was possible to eliminate almost all deviations related to the reference trajectory, reducing the errors to the same scale of the errors generated by the impulsive approach.

4. Conclusion

This work represents an effort in the design of the propulsion system of space vehicles. It was confirmed that the effect of a propulsive arc is not exactly equivalent to the application of an impulse. The difference produces a deviation of the final orbit relative to the reference orbit. This deviation depends on the magnitude of the impulse required for the maneuver, the maximum capacity of the propulsion system and the characteristics of the trajectory control system. Thus, the evaluation of the trajectory deviations is relevant to the analysis of a space mission and in the design of the trajectory control system if a more realistic model is considered instead of the ideal case represented by the impulsive approach. Beyond this, the STRS with the automatic correction of the orbital elements, which utilizes an innovative technology to reduce the errors in the spacecraft path, controlling the continuous thrust in closed loop, was tested with success in the presence of some perturbation forces.

5. References

[1] Battin R H 1999 *An Introduction to the Mathematics and Methods of astrodynamics, Rev. ed.* (Reston: AIAA Educational Series)
[2] Bond V R, Allman M C 1996 *Modern Astrodynamics: fundamentals and perturbation methods* (New Jersey: Princeton University Press)
[3] Rocco E M 2008 Perturbed Orbital Motion with a PID Control System for the Trajectory *XIV Colóquio Brasileiro de Dinâmica Orbital* Águas de Lindóia, November 17 - 21
[4] Rocco E M, Marcelino E W, Prado A F B A, Kuga H K 2010 Closed Loop Control System Applied to Earth-Moon Transfer Maneuvers Using Continuous Thrust *38th Scientific Assembly of the Committee on Space Research* Bremen, Germany, July 18-25
[5] Rocco E. M 2013 Automatic correction of orbital elements using continuous thrust controlled in closed loop *Journal of Physics: Conference Series* **465** doi:10.1088/1742-6596/465/1/012007
[6] Chobotov V A 1991 *Orbital Mechanics* (Washington: American Institute of Aeronautics and Astronautics, Inc.)
[7] Kaula W M 1966 *Theory of Satellite Geodesy Applications of Satellites to Geodesyc* (New York: Blaisdell Pub. Co.)
[8] Lemoine F G, Smith D E, Rowlands D D, Zuber M T, Neumann G A, Chinn D S 2001 An improved solution of the gravity field of Mars (GMM-2B) from Mars Global Surveyor *J. Geophys. Res.* **106** 23359-76
[9] Zuber M T, Lemoine F G, Smith D E, Konopliv A S, Smrekar S E, Asmar S W 2007 Mars Reconnaissance Orbiter Radio Science Gravity Investigation, *J. Geophys. Res*. **112** E05S07, doi:10.1029/2006JE002833
[10] Szebehely V 1967 *Theory of orbits* (New York: Academic Press Inc.)
[11] Edelbanum T N 1961 Propulsion Requirements for Controllable Satellites *ARS Journal* **31** 1079-89
[12] Rocco E M, Souza M L O, Prado A F B A. 2013 Station Keeping of Constellations Using Multiobjective Strategies *Mathematical Problems in Engineering* doi:10.1155/2013/476451